University of South Bohemia

Faculty of Science

Institute of Chemistry and Biochemistry

Bachelor Thesis

Conformational Study of a Flexibility of the Fluorescence Dye QSY21

Filip Zimandl

Supervisor: Mgr.Martin Kabeláč, Ph.D.

České Budějovice 2010

Zimandl, F., 2010, Conformational Study of a Flexibility of the Fluorescence Dye QSY21, Bachelor Thesis in English, 23p., University of South Bohemia, České Budějovice, Czech Republic

Annotation:
This bachelor thesis is focused on a theoretical study of the flexibility of the QSY 21 fluorescence dye. The main aim of this work was to find the most stable conformers of the isolated dye and thus provide the suitable starting structure of the dye for the MD simulation of the QSY 21 bound to the DNA. The torsion barrier between the central xanthene ring and the side ring was evaluated, showing the hindered rotation of the side ring.

Anotace:
Tato bakalářská práce se týká teoretické studie flexibility fluorescenčního barviva QSY 21. Hlavním úkolem práce bylo najít energeticky nejstabilnější konformery ve vodném prostředí a poskytnout tak vhodnou startovní strukturu pro MD simulaci barviva navázaného na DNA. Dále byla spočtena bariéra rotace mezi centrálním xanthenovým kruhem a postranním aromatickým řetězcem. Výpočty prokázaly ve shodě se simulací molekulovou dynamikou, že se jedná o tzv. bráněnou rotaci.

I confirm that I worked out the presented bachelor thesis solely and all the literature used is properly cited.

I hereby declare that, in accordance with Article 47b of Act No. 111/1998 in the valid wording, I agree with the publication of my dissertation thesis, in full / in shortened form resulting from deletion of indicated parts to be kept in the Faculty of Science archive, in electronic form in publicly accessible part of the STAG database operated by the University of South Bohemia in České Budějovice accessible through its web pages.

České Budějovice 24.5.2010

Student’s signature

I am very grateful to my supervisor Dr. Kabeláč for his help. I appreciate his effort. He motivated me and taught me all necessary topics with the big patience. I would like to say thanks also to Mgr. Tomáš Fessl for his advices concerning the experimental background and Dr. Zdeněk Chval for his consultations.

Abbreviations

AO	Atomic Orbital
cc-pVDZ	Correlation-consistent Dunning's basis set of Double Zeta quality
cc-pVTZ	Correlation-consistent Dunning's basis set of Triple Zeta quality
CPCM	Conductor-like Polarizable Continuum Model
CPU	Computer Processor Unit
DFT	Density Functional Theory
DIHI	2,3-dihydro-1-indolyl
DNA	Deoxyribonucleic Acid
FRET	Förster Resonance Energy Transfer
GTO	Gaussian Type Orbital
HF	Hartree-Fock
LCAO	Linear Combination of Atomic Orbitals
LST	Linear Synchrous Transit
MD	Molecular Dynamics
MD/Q	Molecular Dynamics/Quenching
MO	Molecular Orbital
MP	Møller-Plesset
NIR	Near-infrared
PES	Potential Energy Surface
QST	Quadratic Synchrous Transit
QY	Quantum Yield
RI	Resolution of Identity
STO	Slater Type Orbital
STQN	Synchronous Transit-Guided Quasi-Newton
SV(P)	Split Valence basis set containing polarization functions on heavy atoms
TPSS	The exchange functional of Tao, Perdew, Staroverov, and Scuseria
TZVPP	Ahlrichs's Triple Zeta Valence Polarized basis set
SCC-DFTB	Self Consistent Charge Density Fitting Tight Binding

Contents

1 Introduction and an Aim of this Work

A fluorescence spectroscopy is one of the key experimental techniques for a study of processes in living organism. One of the methods of fluorescence spectroscopy, Förster Resonance Energy Transfer (FRET) is extremely useful for an investigation of dynamics processes in cells[1]. FRET is a process involving the radiationless transfer of energy from a donor fluorophore to an appropriately positioned acceptor fluorophore. FRET can occur when the emission spectrum of a donor fluorophore significantly overlaps the absorption spectrum of an acceptor, provided that the donor and acceptor fluorophores dipoles are in favorable mutual orientation. Because the efficiency of energy transfer varies inversely with the sixth power of the distance separating the donor and acceptor fluorophores, the distance over which FRET can occur is limited to below 10 nm.

An usage of fluorescence probes which emit/absorb in near infra-red region is beneficial, since at this spectral region a tissue background signal is eliminated, light near 650 to 900 nm can easier penetrate through the tissue as well as the laser sources are less expensive[2].

For these reasons, many new far-red and near infrared fluorescent probes have appeared on the market, however for most of them the 3-D structure of its binding motif to biomolecules has not been solved yet. The example of these probes is a QSY 21 dye (Figure 1).

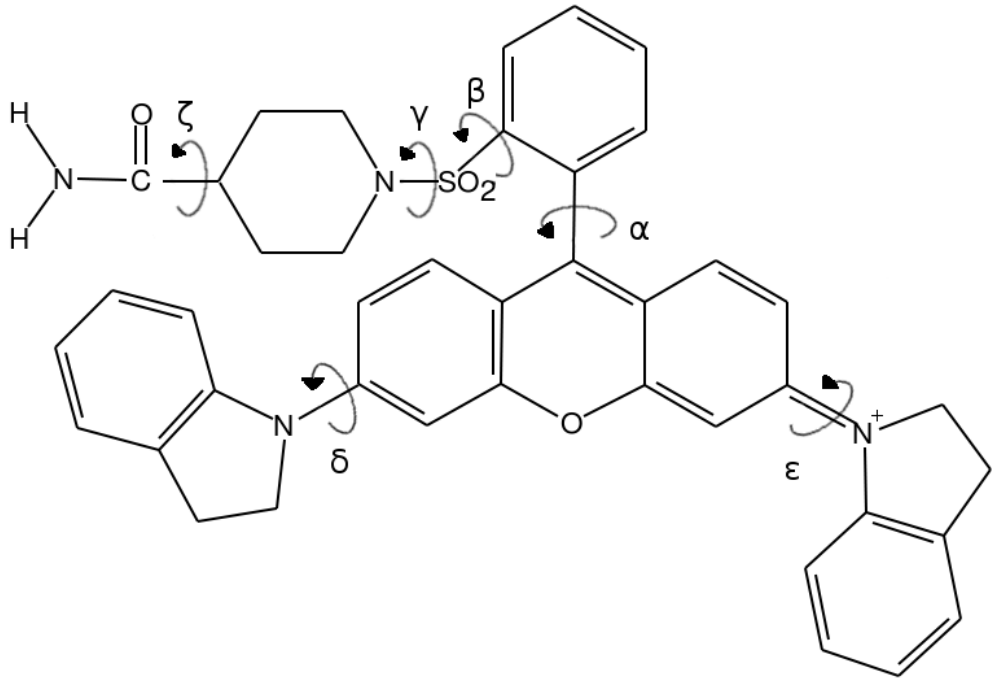

Figure 1. 2-D representation of the QSY 21 fluorescence probe with depicted rotatable bonds.

The QSY 21 is an efficient energy transfer acceptor of the far red and near-infrared fluorescent probes. It works in the wavelength range of 540-750 nm, frequently used in FRET applications[3]. It has suitable spectral characteristics – a molar extinction coefficient of 90000 $cm^{-1}M^{-1}$**,** and the zero quantum yield, meaning that in the normal conditions it does not emit fluorescence (dark quencher). These properties make QSY 21 an excellent FRET acceptor. When the DNA conformation is studied using the fluorescence probes, the QSY 21 probe is covalently bonded to the phosphate group of an adjacent DNA nucleotide via a phosphoramidite linker (Figure 2).

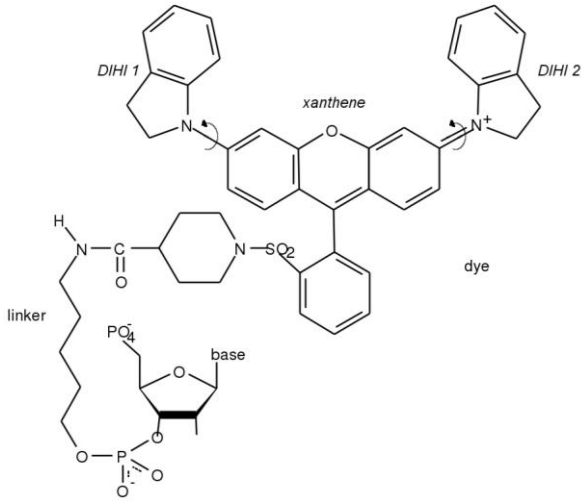

Figure 2. The 2-D representation of QSY 21 probe bonded covalently to the DNA via the aliphatic linker.

Since the binding motif of QSY 21 to the DNA has not been solved yet, the main aim of this work is thus to investigate the structure, dynamics and interactions of the isolated QSY 21 probe and the QSY 21 bound to the B-DNA oligomer using theoretical methods, namely molecular dynamics (MD) and *ab initio* quantum chemical computations. The detailed knowledge of the binding motifs of a probe bound to DNA and of stacking interactions between the probe and the DNA is very important because of the expected changes in probe's photophysical properties upon binding. A key role of the interaction between the probe and guanine should be emphasized. If the possibility of the probe stacking onto guanine is not considered, this interaction could be misinterpreted as a change in donor-acceptor distance.

My contribution to this project was namely focused on the:

1. Conformational flexibility of the isolated QSY 21 probe, i.e. finding the most stable conformers.
2. Estimation of the barrier height of the rotation of most flexible parts of the QSY 21 molecule.

2 Theoretical Background of Quantum Mechanical Methods

Ab initio calculations (*ab initio* is from the Latin: "from the first principles") are based on the Schrödinger equation. This is a one of the fundamental equations of modern physics and it describes, among other things, how the electrons in a molecule behave. A solution of the Schrödinger equation (Eq. 1, 2) for a molecule and gives us the molecule's energy (or other property) from the wavefunction Ψ.

$$E\psi(r) = -\frac{\hbar^2}{2m}\nabla^2(r) + V(r)\psi(r) \tag{1}$$

The differential operator ∇ has a form:

$$\nabla = \frac{\partial}{x} + \frac{\partial}{y} + \frac{\partial}{z} \tag{2}$$

The mass is expressed as *m* and ħ is reduced Planck constant.

Using the condensed form of the Hamiltonian operator $\hat{H}$, the total energy can be obtained from the equation:

$$\hat{\mathcal{H}}\psi = E\psi \tag{3}$$

The Schrödinger equation, however, cannot be solved exactly for any molecule with more than one electron. Thus approximations are used; the less serious these are, the "higher" the level of the *ab-initio* calculation is said to be. Regardless of its level, an *ab initio* calculation is based only on basic physical theory (quantum mechanics) and is in this sense "from the first principles". *Ab-initio* calculations are relatively slow and affordable only for systems to approximately 100 of atoms.

2.1. Mathematical and Physical Approximations used in the Solution of the Schrödinger Equation

2.1.1 Neglecting of Relativistic Effect

A relativistic effect influences the electron's properties therefore also on the energy.

It comes from the inclusion of the Einstein's Theory of relativity. The Quantum Mechanics has been originally developed in a non-relativistic way. This effect in quantum chemistry can be important for heavier elements. For the majority of calculations in biology this

effect is neglected and we use non-relativistic Schrödinger equation.

2.1.2 Born-Oppenheimer Approximation

This approximation is based on fact that electrons are much lighter than protons and neutrons. The movement of the nucleus is quite negligible in contrast with the speed of electrons, therefore the nucleus is treated as static. The total molecular wave-function can be thus splitted into two components, electronic and nuclear ones:

$$\psi_{total} = \psi_{electronic} \times \psi_{nuclear} \tag{4}$$

2.1.3 Model of Independent Electrons – Central Field Approximation

The aim of this approximation is to replace the original wave-function dependent on coordinates of all electrons by the system of equations dependent only on coordinates of one-electron, in which this electron moves in an average electric field of the other electrons and nuclei. The simplest wave-function for a description of the ground state of the molecule with N electrons satisfying the Pauli's principle is expressed in a form of a single Slater determinant:

$$\psi(x_1, x_2, \ldots, x_N) = \frac{1}{\sqrt{N!}} \begin{vmatrix} \chi_1(x_1) & \chi_2(x_1) & \ldots & \chi_N(x_1) \\ \chi_1(x_2) & \chi_2(x_2) & \ldots & \chi_N(x_2) \\ \vdots & \vdots & & \vdots \\ \chi_1(x_N) & \chi_2(x_N) & \ldots & \chi_N(x_N) \end{vmatrix} \tag{5}$$

where χ is a given atomic spin orbital and the term (6) is a normalization factor.

$$\frac{1}{\sqrt{N!}} \tag{6}$$

2.1.4. Molecular Orbital - Linear Combination of the Atomic Orbitals (MO-LCAO)

Molecular orbital (MO) is a one-electron wave-function for an electron that spreads throughout the molecule. To simplify our calculations, the MOs are constructed from linear combinations of the atomic orbitals.

$$\phi_i = \sum_r c_{ri}\chi_r \tag{7}$$

where χ_r is set of basis function describing atomic orbital, Φ_i is a molecular orbital description and c_{ri} is coefficient.

2.2 Basis Set

Basis set is a set of mathematical functions which describe atomic orbitals. In principle any type of basis function may be used: exponential, Gaussian, polynomial, cube, plane wave etc[4]. The two most common types of orbitals are Slater type orbital (STO) and Gaussian type orbital (GTO). The shapes of primitive Gaussian and Slater type functions are shown in Figure 3 (mathematical expressions of these functions in Cartesian coordinates are written as Eq. 8 and 9). Atomic orbitals were originally represented as Slater type orbital due to their similarity with the eigenfunctions of the hydrogen atom. However due to non-existence of the analytical solutions of the integrals containing the Slater's functions, the sets of the Gaussian functions are rather used.

$$\psi_{n,l,m,\zeta}(r,\theta,\phi) = f(r,\theta,\phi) \times e^{-\zeta r^2} \tag{8}$$

$$\psi_{n,l,m,\zeta}(r,\theta,\phi) = f(r,\theta,\phi) \times e^{-\zeta r} \tag{9}$$

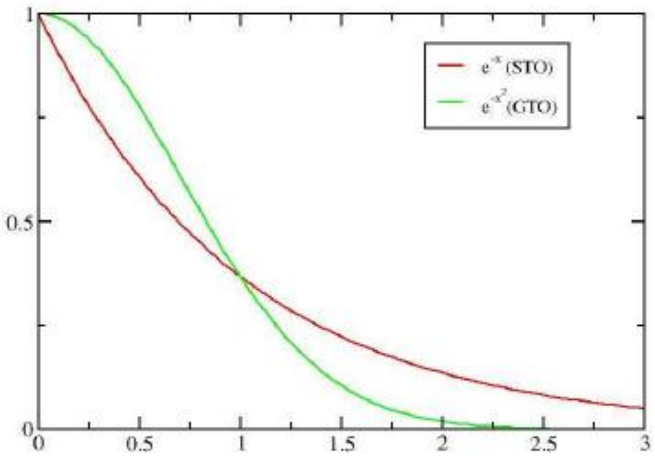

Figure 3. The Slater and Gaussian function.

2.3 Ab-initio Calculations

2.3.1 Hartree-Fock Method

The Hartree-Fock method (HF) is based on an approximative solution of the Schrődinger equation using approximations briefly described in the Section 2. The total molecular wavefunction is approximated as a Slater determinant composed of occupied spin orbitals (each spin orbital is a product of a conventional spatial orbital and a spin function). The spatial orbitals are approximated as a linear combination (a weighted sum) of basis functions. These functions describe the atomic orbitals. The main defect of the HF method is that it does not treat electron correlation properly: each electron is considered to move in an electrostatic field represented by the average positions of the other electrons, whereas in fact electrons avoid each other better than the HF method predicts.

HF is the simplest and fastest *ab-initio* method but it does not cover the correlation energy (except the exchange term). The electron correlation energy is the difference of the energy between the HF limit (energy calculated with the infinite basis set) and the exact solution of the non-relativistic Schrödinger equation. The HF calculation is a central point for a majority of quantum chemical methods which goes beyond the HF one, or are simpler than the HF one (semiempirical methods).

2.3.2 Møller-Plesset Perturbation Theory

The Møller-Plesset method (MP) represents one of the simplest approaches for going beyond the Hartree-Fock approximation to obtain the correlation energy. The principle of this method is to divide the total Hamiltonian into two parts, the zeroth-order part (H_0) and a perturbation V. H_0 is the Hartree-Fock Hamiltonian. The first correction to the Hartree-Fock energy occurs in the second order of the perturbation theory and it involves a sum over doubly excited determinants. These can be generated by promoting two electrons from occupied orbitals to virtual orbitals.

MP2 typically accounts for ≈ 80-90% of the correlation energy, and it is the most economical method for including electron correlation. Higher orders of the perturbation theory are not widely used.

2.3.3. Density Functional Theory (DFT)

The DFT is an another approach in computational chemistry. The basis of the DFT method is the proof by Hohenberg and Kohn[5] that the ground-state electronic energy is determined completely by the electron density ρ. The electron density is the square of the wave function and it depends on three coordinates, independently of the number of electrons. The "only" problem is that the exact functional connecting the energy (or the other physical properties) and the electron density is not known precisely. Nowadays DFT is a leading method due to comparable accuracy to *ab-initio* calculations, but with less demanding computational cost. Sometimes is considered as the *ab-initio* theory, however it is not, since it includes some empirical approximation terms. DFT as well as HF does not cover the dispersion energy, thus an extra term which covers the dispersion energy in empirical way[6] is added when required.

2.3.4. Self-Consistent-Charge Density Functional Tight-Binding Method (SCC-DF-TB-D)

The Self-consistent-charge density functional tight-binding method[7] covers the dispersion term and it is an approximate quantum chemical method derived from the DFT belonging to the semiempirical methods. It is very fast in comparison with the standard DFT methods, however it is still quite reliable for a study of biological systems.

2.4. Searching for Minima on the Potential Energy Surface of the Molecule

The flexible systems containing higher amount of the rotatable bonds are characterized by the multiple minima on the molecular surface. Standard minimization algorithms (steepest descent, conjugated gradient…) tend to fall to the closest local minimum energy conformation, therefore they cannot overcome the energy barriers between two minima. Thus it is desirable to use more sophisticated method to locate all energy minima at the potential energy surface.

In a grid search method all rotatable bonds in the molecule are identified. Each of these bonds is then systematically rotated through 360 degrees using a fixed increment. Every generated conformation is minimized to obtain the associated minimum. The search stops when all possible combinations of torsion angles have been generated and minimized.
Oppositely, using the random search method we randomly change the geometrical parameters of our studied molecule and the structure minimization is further employed. The Metropolis Monte Carlo scheme is often used to generate random structures. The usual strategy is to generate conformations until no new structures can be obtained.

In our work we are going to use the combination of molecular dynamics
and molecular mechanics, so called Quenched Molecular dynamics, which is going to be described in the following section.

2.4.1 Quenched Molecular Dynamics (MD/Q)

A classical molecular dynamics applies the Newton's laws of motion to describe the movement of the molecules. A common strategy of MD/Q is to perform the dynamics at a very high, physically unrealistic temperature. The excess of the kinetic energy enhances the ability of the system to overcome the energy barriers and thus it can prevent the molecule getting stuck in a small region of conformational space.

This procedure is schematically illustrated in the Figure 4. The MD structures are then selected at regular intervals from the trajectory for subsequent energy minimizations.

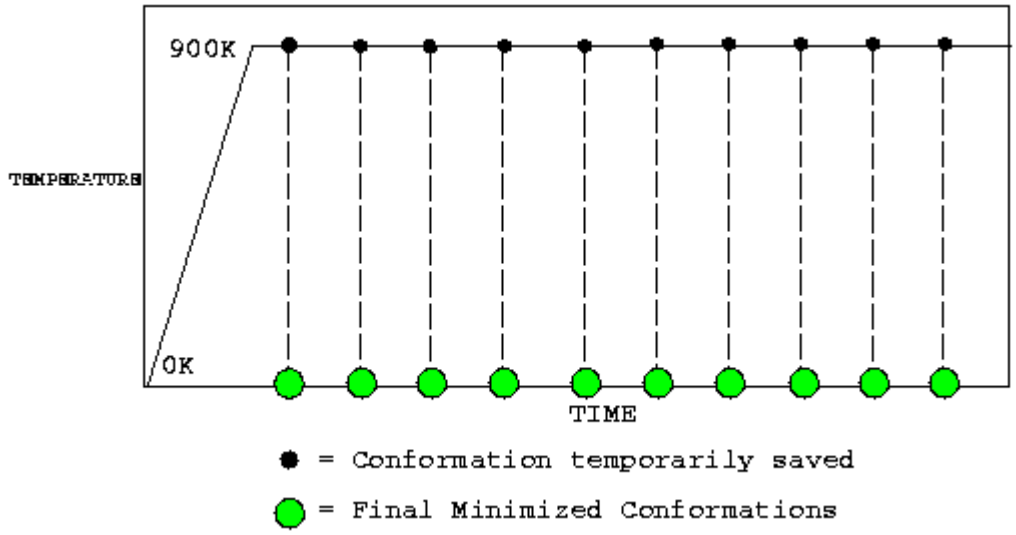

Figure 4. A schematic representation of MD/Q procedure.

2.5. Searching for the Transition State Structures

Transition state of a chemical reaction/rotational barrier corresponds to a saddle point on the potential energy surface. Searching for the transition state is more difficult than for a local minimum. One needs to provide a rather good guess in order for the optimization procedure to converge. For this reason, finding the transition state is not always trivial, particularly for large molecular systems. Once the transition state is located or optimized, it should be confirmed by performing a vibrational analysis. A saddle point should have one imaginary frequency (often printed as negative value by many quantum chemistry programs) and its vibrational mode should correspond to the motion that connects the reactant and product.

The simplest way to guess the shape of a transition structure is to assume that each atom is directly between the position where it starts (reactant) and the position where it ends (product). This linear motion approximation is called linear synchronous transit (LST). This is a good first approximation, but it has its failings. Consider the motion of an atom which is changing bond angle with respect to the rest of the molecule. The point half way between its starting and ending positions on the line connecting those positions will give a shorter than expected bond length and thus be (perhaps significantly) higher in energy.

The logical extension of this technique is the quadratic synchronous transit method (QST). This method assumes the coordinates of the atoms in the transition structure will lie along a parabola connecting the reactant and product geometries.

3 Methods

3.1 Molecular Dynamics/Quenching (MD/Q) Calculations of Isolated Dye

Employing the approximate self-consistent-charge, density functional tight-binding method with the inclusion of an empirical dispersion term (SCC-DF-TB-D)[8], the potential energy landscape of QSY 21 dye (Figure 1) was explored using the MD/Q approach[9]. The initial distribution of atomic velocities was evaluated by using Andersen stochastic algorithm[10], temperature was held constant at 900K during the whole MD run (NVT ensemble). The total length of the MD part was 1 ns with the integration time step of 0.5 fs. Each 20000th frame had been saved for further nonrestricted minimization by the same method using the steepest descent algorithm. After performing the MD/Q run, all the optimized conformers were sorted on the basis of their energies and geometries. This procedure, and bearing into mind the system symmetry reduced, the initial set of energy minimized structures to a set of geometrically distinct structures, which correspond, with a high probability, to all the existing minima of the probed part of PES. The torsion angles responsible for the flexibility of the molecule are depicted in Figure 1.

3.2 Correlated Ab-Initio Quantum Chemical Calculations of Isolated Dye

Each 100th structure of the conformers obtained by the MD/Q/SCC-DF-TB-D method was further optimized at the *ab-initio* level of theory. The optimizations were performed with the Resolution of Identity (RI-)DFT-D (TPSS hybrid functional[11] with an empirical dispersion term)[12] method employing the SVP basis set. The six most geometrically distinct structures were further reoptimized at the same level of theory with TZVPP basis set. The actual calculations were performed using the Turbomole 6.0 program package[13].

3.3. Estimation of Rotational Barrier Height of DIHI Rings

Since the largest flexibility in the molecule was observed for the rotation of two 2,3-dihydro-1-indolyl rings (DIHI) with respect to xanthene ring, we were interested in the estimation of barrier height of this rotation. We used a model system of DIHI-benzene (Figure 5) to greatly reduce the total CPU time during the calculations without loosing accuracy in comparison with the QSY 21 dye. At first, a rigid scan had been performed by using just single point calculations. After this procedure we had known the approximate values of angles corresponding to the minima at the potential energy surface. Further, the fully relaxed optimizations of minima and transition states were performed at DFT (TPSS functional) and MP2 levels of theory employing the cc-pVDZ and cc-pVTZ Dunning's basis sets[14] in the vacuum, as well as at the implicit solvent, namely using Conductor-like Polarizable Continuum Model (CPCM) mimicking the aqueous surrounding. Transition states were found by the Synchronous Transit-Guided Quasi-Newton (STQN) method. This method uses quadratic synchronous transit approach to get closer to the quadratic region around the transition state and then uses a quasi-Newton algorithm to complete the optimization. Minima and desired transition states were confirmed by the harmonic frequency analysis. The Gaussian 03 program package[15] was used for this part of calculations.

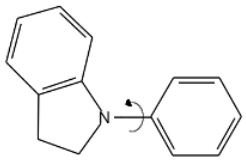

Figure 5. The structure of 2,3-dihydro-1-indolyl benzene with a rotatable bond depicted.

4 Results and Discussion

4.1 Conformational Flexibility of the QSY 21 Dye.

The minimization of the structures at the RI-DFT level of theory did not produce significant geometry changes in comparison with the SCC-DF-TB-D ones. The energetically and geometrically similar structures were sorted according to their energies and to the characteristic torsion angles corresponding to the rotatable bonds in the molecule (Figure 1). Considering the system symmetry we revealed totally about 30 (depends on the angle's threshold) geometrically or energetically distinguishable structures. The six most geometrically distinct structures were further reoptimized at the same level of theory with the TZVPP basis set.

These six conformers are depicted in the Figure 6 and their energetic and geometrical characteristics can be found in the Table 1. These 6 structures were proven as minima by the standard harmonic vibrational analysis.

The most stable conformers corresponds to the structure, where the N-H…π interaction between the terminal NH_2 and one of DIHI rings is observed. The easiest conformational change of the molecule corresponds to the rotation of two DIHI rings (see structures A and B; torsions δ and ε) with respect to the xanthene central ring. The energy differences between such rotamers are very small (systematically 0.1-0.4 kcal/mol, but with respect to the relative representation none of these conformations is preferable). The equilibrium value of the torsion angles is about 10-20 degrees shifted in majority structures in comparison with the planar conformation representing the energy maxima (except the structure C, characterized by the δ torsion angle value ~33degrees) Due to such small difference in energy, only one rotamer corresponding to the most stable combination of above mentioned torsion angles δ and ε will be further discussed.

The rotation of the bond between the sulphonyl group and the phenyl ring is mainly responsible for the flexibility of the non-aromatic part of the molecule (the torsion β in Figure 1 and Table 1). The equilibrium value between 120-140 degrees for structures A-D corresponds to the closest contact between non-aromatic part and the aromatic DIHI ring. The structures E and F possessing torsion angle far from this optimal value of the torsion angle β are much less stable than the structure of the global minimum. When the amidic

group became even more distant apart of DIHI ring (structure E), the decrease in stability by about 3 kcal/mol in comparison with the most stable structure is observed. Finally, pointing the aliphatic part of the molecule perpendicularly (β angle close to zero) to the xanthene ring; (structure F), leads to the least stable conformer being almost 6 kcal/mol less stable than the structure of the global minimum.

Reorientation of the terminal amidic group (compare structures C and D; the ζ torsion 287 respectively 232 degrees) leads to the preference the opposite orientation of the neighbor DIHI ring in these two cases. These two conformers are by about 1.5 kcal/mol less stable than the global minimum.

The rotation around the torsion angles α and γ is highly probably strongly hindered, since the almost same values of these torsion angles for all structures found were observed.

Table 1. The relative energies (in kcal/mol) and the geometrical characteristics (for the definition of the torsion angles see Figure 1) of the six most stable conformers of the isolated QSY 21 probe.

Structure	Energy (kcal/mol)	α	β	γ	δ	ε	ζ
A	0.00	269.1	120.3	279.4	8.2	195.4	324.4
B	0.24	268.1	119.5	280.1	8.5	163.4	325.1
C	1.63	281.1	135.4	281.2	326.7	194.6	287.5
D	1.98	286.1	141.8	279.9	18.6	196.4	232.4
E	2.88	289.3	86.0	296.1	339.4	196.5	312.8
F	5.73	259.2	349.7	292.4	20.0	196.6	239.6

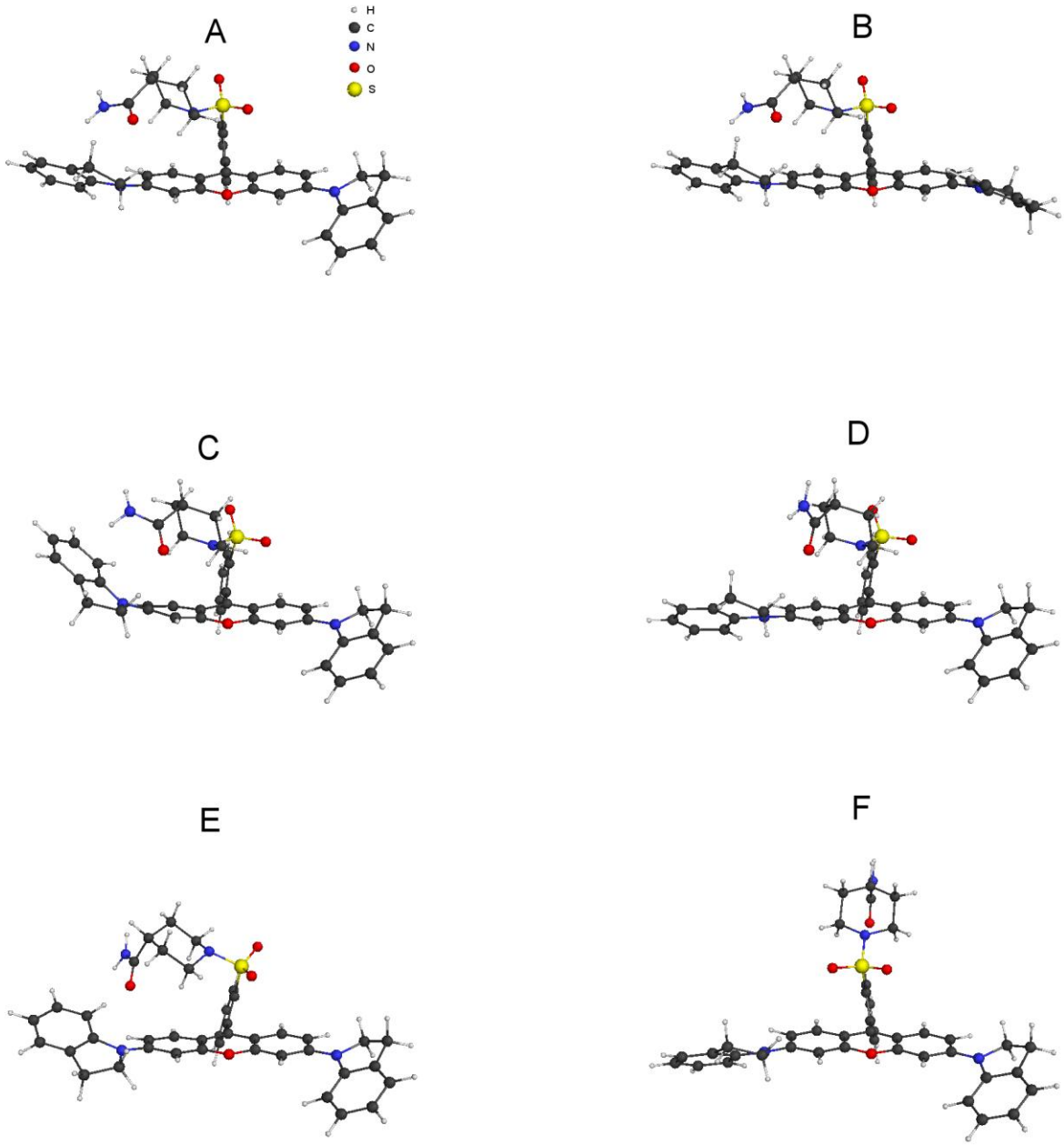

Figure 6. The six most stable conformers of the isolated QSY 21 probe.

4.2. The Rotation Barriers of the QSY 21 Aromatic Side Ring

As we demonstrated at the previous paragraph, the largest flexibility of the isolated QSY 21 molecule corresponds to the rotation of the DIHI rings. Further, the DIHI side rings of the QSY 21 significantly contribute to the stabilization of the DNA-QSY 21 complex, as it can be seen in the MD simulation (See Appendix A). Thus, the knowledge of the energy barrier of the rotation of the DIHI ring in terms of the main xanthene ring would be beneficial. To estimate the barrier height we used a model structure, 2,3-dihydro-1-indolyl benzene (Figure 5).

Our model is similar to the biphenyl molecule, which has been extensively studied both experimentally and theoretically. Recent experimental studies indicate that the energy barriers separating the minimum from the planar and perpendicular arrangements of biphenyl are nearly the same, corresponding to the values of 1.4 and 1.6 kcal/mol respectively, with the equilibrium torsion angle of 44.4°. Even the highest level *ab-initio* methods have a tendency to overestimate slightly the barriers, namely by about 0.5 kcal/mol.

Our results for the rotation of the DIHI ring in the QSY 21 show that the structure of the minimum is characterized by the torsion angle of 41.4° calculated at the MP2/cc-pVTZ level of theory (See Figure 7 and Table 2). The barrier is slightly larger than for the biphenyl molecule: 3.63 kcal/mol (the corresponding equilibrium angle is -11.2°) for the "planar" form and 2.09 kcal/mol (equilibrium angle 80.6°) for the "perpendicular" form. The analogous data for biphenyl correspond to the values of 2.39 and 2.04 kcal/mol, respectively. These values suggest a hindered rotation of the DIHI ring in the QSY 21 molecule. The role of the ZPVE energy is marginal, leading to a correction in the relative barrier heights of less than 0.1 kcal/mol.

When the DFT calculation is applied, an exchange in order of barrier heights was observed. This rather erratic behavior is generally explained by overstabilization of planar π-conjugated conformers by DFT methods[16].

Not even the effect of the environment is crucial. The rotation barrier is systematically smaller by 0.2-0.3 kcal/mol in implicit water than in vacuum despite the high-level method and basis set used (Table 2).

These conclusions are fully confirmed by the distribution and the time evolution of

the torsion angles in the course of the MD simulation (Compare top and bottom part of the Figure 7). In the conformational states where the side ring is not stacked, it rotates around the linker bond. The rotation is not entirely free, but the barriers are rather low. This is indicated by the fast transitions among the rotation substates, the lifetime of each substate being of the order of 100 ps to 1 ns. Moreover, the most populated rotation substates correspond to the energy minima as revealed by the QM calculations. The low rotation barriers ensure a good adaptation of the torsion angle in those states where the side ring is stacked, so that the stacking is close to optimal and not compromised by the torsion angle barriers.

Table 2. An energy profile of the rotation of the DIHI ring employing various method and basis set in vacuum and in the implicit water. Torsion angles are in degrees, relative energies in kcal/mol.

MP2/cc-pVDZ				MP2/cc-pVTZ			
vacuum		water		vacuum		water	
torsion	ΔE	torsion	ΔE	torsion	ΔE	torsion	ΔE
4.6	4.37	4.1	4.00	-11.4	3.63	-11.7	3.30
48.5	0.00	47.9	0.00	41.6	0.00	40.9	0.00
83.9	1.54	83.0	1.38	80.6	2.09	80.4	1.84
151.5	0.00	151.1	0.00	136.9	0.00	136.5	0.00
184.6	4.37	184.1	4.00	168.6	3.63	168.3	3.30
228.5	0.00	227.9	0.00	221.6	0.00	220.9	0.00
263.9	1.54	263.0	1.38	260.6	2.09	260.4	1.84
331.5	0.00	330.9	0.00	316.5	0.00	316.0	0.00

TPSS/cc-pVDZ				TPSS/cc-pVTZ			
vacuum		water		vacuum		water	
torsion	ΔE	torsion	ΔE	torsion	ΔE	torsion	ΔE
0.0	2.39	0.0	2.07	0.0	2.13	0.0	1.84
33.6	0.00	33.5	0.00	28.3	0.00	28.4	0.00
76.9	3.19	76.4	3.02	73.8	3.63	72.5	3.36
149.4	0.00	149.5	0.00	151.7	0.00	151.6	0.00
180.0	2.39	180.0	2.07	180.0	2.13	180.0	1.84
210.6	0.00	210.6	0.00	208.3	0.00	208.4	0.00
256.5	3.19	255.7	3.02	253.8	3.63	252.5	3.36
326.4	0.00	326.5	0.00	328.8	0.00	328.7	0.00

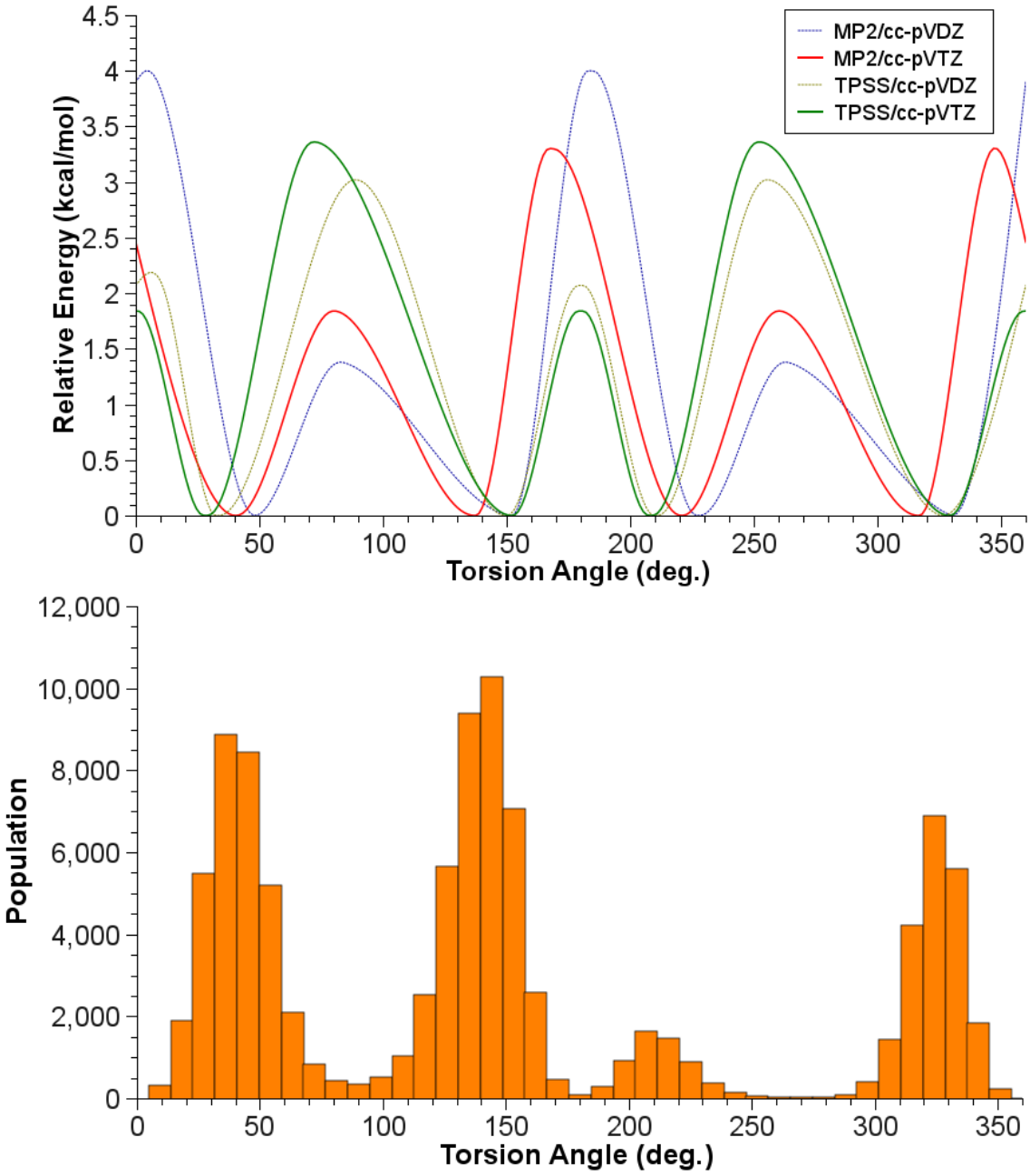

Figure 7. Calculated energy profile of a rotation of the DIHI ring using different methods (top) compared with the distribution of the torsion angles of the DIHI ring during the MD simulation (bottom).

5. Conclusions

We employed the MD/Q method to locate the minima of the isolated QSY21 dye. More than 30 conformers were found and 6 lowest-lying structures were further reoptimized at the high level *ab-initio* methods. The energy differences between the four most stable structures are rather small, not exceeding 2 kcal/mol. The largest flexibility in the molecule corresponds to the rotation of the DIHI ring. The structure of the global energy minimum was further employed in the initial structure of QSY 21 bonded covalently to the DNA in the MD simulation.

The calculated energy barriers of the rotation of the DIHI ring are in the very good agreement with the MD simulation. The barrier height is around 3 kcal/mol (slightly higher than for the biphenyl molecule), what corresponds to the hindered rotation of the bond. From the MD simulation it is obvious that this rotation is not entirely free. Moreover, the positions of the maxima/minima at the energy profile of the rotation calculated by quantum mechanical calculations are in concert with the distribution of the torsion angles from the MD simulation.

These conclusions as well as the binding motifs found by MD simulation can shed a light on the interaction of the novel fluorescence probe QSY 21 with DNA and thus help the experimentalist with the interpretation of their results.

6. References

1. C. L. Takanishi, E. A. Bykova, W. Cheng, J. Zheng, *Brain Res.* 2006, **1091** (1), 132-139.
2. C. L. Amiot, S. Xu, S. Liang, L. Pan, *Sensors-Basels* 2008**, 8**, 3082-3105.
3. H. Neubauer, N. Gaiko, S. Berger, J. Schaffer, C. Eggeling, J. Tuma, L. Verdier, C. A. Seidel, C. Griesinger and A. Volkmer, *J. Am. Chem. Soc.* 2007, **129**, 12746-12755.
4. Jensen, Frank, *Introduction to Computational Chemistry* **1999**, Chichester, England: John Wiley and Sons. 150–176. ISBN 0471984156.
5. P. Hohenberg and W. Kohn, *Phys. Rev. B.* 1964, **136B**, 864.
6. S. Grimme, *J. Comput. Chem.* 2004, **25,** 1463-1473.
7. M.Elster, *Theor. Chem. Acc.* 2006, **116,** 316-325.
8. M. Elstner, T. Frauenheim, E. Kaxiras, G. Seifert, S. Suhai, *Phys. Status Solidi B.* 2000**, 217** (1), 357-376.
9. F. G. Amar, R. S. Berry, *J. Chem. Phys.* 1986**, 85** (10), 5943-5954.
10. Hans C. Andersen, *J. Chem. Phys.* 1980, **72**, 2384-2393.
11. J. M. Tao, J. P. Perdew, V. N. Staroverov and G. E. Scuseria, *Phys. Rev. Lett.* 2003, **91**, 146401-146404.
12. Antony, J.; S. Grimme, *Phys. Chem. Chem. Phys.* 2006, **8** (45), 5287-5293.
13. R. Ahlrichs, M. Bar, M. Haser, H. Horn, C. Kolmel, *Chem. Phys. Lett.* 1989, **162** (3), 165-169.
14. T.H. Dunning, *J. Chem. Phys.* 1989, **90**, 1007-1023.
15. M. J. Frisch, G. W. Trucks, H. B. Schlegel, G. E. Scuseria, M. A. Robb, J. R. Cheeseman, J. A. Montgomery, T. Vreven, K. N. Kudin, J. C. Burant, J. M. Millam, S. S. Iyengar, J. Tomasi, V. Barone, B. Mennucci, M. Cossi, G. Scalmani, N. Rega, G. A. Petersson, H. Nakatsuji, M. Hada, M. Ehara, K. Toyota, R. Fukuda, J.

Hasegawa, M. Ishida, T. Nakajima, Y. Honda, O. Kitao, H. Nakai, M. Klene, X. Li, J. E. Knox, H. P. Hratchian, J. B. Cross, V. Bakken, C. Adamo, J. Jaramillo, R. Gomperts, R. E. Stratmann, O. Yazyev, A. J. Austin, R. Cammi, C. Pomelli, J. W. Ochterski, P. Y. Ayala, K. Morokuma, G. A. Voth, P. Salvador, J. J. Dannenberg, V. G. Zakrzewski, S. Dapprich, A. D. Daniels, M. C. Strain, O. Farkas, D. K. Malick, A. D. Rabuck, K. Raghavachari, J. B. Foresman, J. V. Ortiz, Q. Cui, A. G. Baboul, S. Clifford, J. Cioslowski, B. B. Stefanov, G. Liu, A. Liashenko, P. Piskorz, I. Komaromi, R. L. Martin, D. J. Fox, T. Keith, A. Laham, C. Y. Peng, A. Nanayakkara, M. Challacombe, P. M. W. Gill, B. Johnson, W. Chen, M. W. Wong, C. Gonzalez and J. A. Pople, Gaussian 03, Revision C.02, 2003.

16. A. Karpfen, C.H. Choi and M. Kertesz, *J. Phys. Chem. A.* 1997, **101**, 7426-7433.

Appendix A

A Comparative Study of the Binding of QSY 21 and Rhodamine 6G Fluorescence Probes to DNA: Structure and Dynamics

Martin Kabeláč, Filip Zimandl, Tomáš Fessl, Zdeněk Chval and Filip Lankaš

Phys. Chem. Chem. Phys.*, 2010, DOI:10.1039/c004020g, *in press